

Artificial Equilibrium Points for a Solar Balloon in the Alpha Centauri System

Generoso Aliasi, Giovanni Mengali, Alessandro A. Quarta*

Department of Civil and Industrial Engineering, University of Pisa, I-56122 Pisa, Italy

Abstract

This paper discusses the generation, stability, and control of artificial equilibrium points for a solar balloon spacecraft in the α Centauri A and B binary star system. The continuous propulsive acceleration provided by a solar balloon is shown to be able of modifying the position of the (classical) Lagrangian equilibrium points of the three-body system on a locus whose geometrical form is known analytically. A linear stability analysis reveals that the new generated equilibrium points are usually unstable, but part of them can be stabilized with a simple feedback control logic.

Key words: Solar balloon, Artificial equilibrium points, Alpha Centauri binary star system

Nomenclature

a	=	semimajor axis of stars' orbit
\mathbf{a}_P	=	propulsive acceleration
C	=	center of mass

* Corresponding author.

Email addresses: g.aliasi@dia.unipi.it (Generoso Aliasi), g.mengali@ing.unipi.it
(Giovanni Mengali), a.quarta@ing.unipi.it (Alessandro A. Quarta).

c	=	speed of light
d_ρ, d_i, d_k	=	auxiliary variable, see Eqs. (10)–(12)
\mathbf{E}, \mathbf{K}	=	second order tensors, see Eqs. (19) and (18)
\mathbb{E}, \mathbb{K}	=	matrix representation in \mathcal{T}_p of tensors \mathbf{E}, \mathbf{K}
e	=	eccentricity of stars' orbit
G	=	universal gravitational constant
g	=	auxiliary variable
h_P, h_D	=	proportional-derivative controller gains
$\hat{\mathbf{i}}, \hat{\mathbf{j}}, \hat{\mathbf{k}}$	=	unit vectors of rotating frame
L	=	luminosity
$L_i, i = 1 \dots 5$	=	Lagrangian equilibrium points
ℓ	=	distance between α Cen A and B
k_{22}	=	\mathbb{K} -matrix entry, see Eq. (23)
m	=	mass
\mathbb{O}, \mathbb{I}	=	zero and identity matrices
R	=	balloon's nominal radius
\mathbf{r}	=	position vector, $r = \ \mathbf{r}\ $
T	=	period of stars' orbit
\mathbb{U}	=	matrix representation in \mathcal{T}_p of vector \mathbf{u}
\mathbf{u}	=	input vector, see Eq. (20)
x, y, z	=	coordinates in the rotating reference frame
β	=	sail lightness number
δ	=	variation
ε	=	auxiliary variable, see Eq. (6)
η	=	sail efficiency
μ	=	dimensionless mass of α Cen B

ν	=	true anomaly of α Cen B
$\boldsymbol{\rho}$	=	relative position vector, $\rho = \ \boldsymbol{\rho}\ $
\mathcal{T}	=	reference frame
$\boldsymbol{\omega}$	=	angular velocity, $\omega = \ \boldsymbol{\omega}\ $

Subscripts

0	=	equilibrium condition
A	=	α Cen A
B	=	α Cen B
M	=	point M , see Fig. 4(a)
max	=	maximum
p	=	pulsating reference frame
\odot	=	Sun

Superscripts

'	=	derivative with respect to ν
T	=	transpose

1 Introduction

The α Centauri system (see Fig. 1) is composed by a binary subsystem of solar-like stars, namely, α Cen A and B, orbited by a red dwarf star (Proxima Centauri) at about 15000 au away from the center of mass of the other two celestial bodies [1,2]. At a distance of about

1.35 pc from the Sun, such a system is the closest to the our star, and its proximity makes it the natural target for the first interstellar spacecraft missions in the future.

A significant scientific interest drives the study of this binary star system. This is mainly due to the analogies of α Cen A and B with the Sun. In fact, α Cen A and B are stars of type G2V and K1V, respectively, which belong to the main sequence and have masses similar to the Sun's mass. Moreover α Cen A and B are high-metallicity stars, which would promote the existence of circumstellar discs and the formation of Earth-like planets [3,4]. Therefore, on one side the study of α Cen A and B represents a fundamental step for understanding the structure and evolution of the Solar System, on the other side the similarity of the two stars with the Sun could simplify the discovery of Earth-twin exoplanets within the binary system [2,4,5]. The latter aspect is very intriguing, especially if new discovered planets orbit in the so-called habitable zone of the system. In fact, in that case the large number of binary and multiple systems in the galaxies would imply a large number of potentially habitable extrasolar planets [6].

From the point of view of a spacecraft mission analysis, Proxima and α Cen A and B can be considered as two separate star systems, being Proxima small and far away from the other two stars, see Fig. 1. Therefore, the motion of the spacecraft near the α Centauri binary system can be treated using a (restricted) three-body gravitational model [7,8]. Within such a model, interesting possibilities for observational missions of both stars are offered by the Artificial Equilibrium Points (AEPs), which can be generated by displacing the position of the classical Lagrangian points by means of a suitable continuous propulsive acceleration [9]. In particular, a suitable choice for a candidate observational mission could be one of the points located along the segment between the two stars (referred to as L_1 -type points), as these points enhance the capability of observing simultaneously the two stars and their possible planets from similar distances. In this sense, and for a preliminary observational mission, the middle point of the segment seems to be a reasonable candidate for obtaining data from both stars.

As far as the propulsion system is concerned, a propellantless propulsion concept represents the natural choice to enable a long-life mission. In this respect solar sailing has received considerable attention in the last few years for both planetary and deep space missions [10,11], in particular after the recent successes of Japanese IKAROS (Interplanetary Kite-craft Accelerated by Radiation Of the Sun) mission, which has started to show the concrete advantages of a propellantless propulsion system in an interplanetary trajectory. The choice of a propellantless propulsion system is also worthwhile because it guarantees the possibility of a continuous control to stabilize the equilibrium points. In particular, solar sails are known to enable the use of a simple control strategy, referred to as β -control, see Ref. [12].

In most cases, AEPs generated by solar sails have been investigated under the assumption of a single source of light [9,10,13], whereas the generation of AEPs in the α Cen A and B requires the introduction of a double source of radiation pressure. The latter case has been partially discussed in a few cases only [14,15,16,17]. In general, previous works deal with the photogravitational (circular or elliptic) three-body problem when two generic radiating celestial bodies are involved. In particular, Simmons et al. [14] studied the circular problem with two radiating bodies. In their work they showed that up to nine different equilibrium points could exist, and they found the locus where the equilibrium points could stay, when both luminosities and masses of the radiating bodies are varied. Markellos et al. [15,16,17] extended the work of Simmons et al. [14], by studying the stability of the equilibrium points in the elliptic problem with two radiating bodies.

This paper investigates the generation, stability, and control of AEPs for a solar sail based spacecraft within the α Cen A and B system as an extension of previous works [9,18] where only one radiating body is taken into account. The two stars are now treated with different luminosities, thus providing a more realistic model of the actual environment where the spacecraft will be placed. From this viewpoint the present work extends the results about collinear AEPs obtained by Markellos et al. [17] under the assumption of two stars having the same luminosity.

The spacecraft is assumed to be a solar balloon [12,19], which is constituted by a thin spherical shell with a reflective surface inflated through a suitable gas. A solar balloon essentially behaves like a spherical solar sail, providing a purely radial thrust with respect to each of the two radiation sources. It is possible to show that two different families of AEPs exist when a solar balloon is used as the primary propulsion system, and the performance necessary to the spacecraft for creating and maintaining an AEP can be calculated. Finally a linear stability analysis is also provided, and the effects of a Proportional-Derivative (PD) control law are discussed for a type of AEPs that are interesting for observational missions. The introduction of a control strategy for the AEPs also represents a further improvement over the previous works [17].

1.1 Dynamical model

Under the assumption that the photogravitational effects of Proxima are negligible, the motion of a solar balloon spacecraft in the α Centaury system can be described within an elliptic restricted three-body problem. In this system α Cen A and α Cen B are the two primaries of mass $m_A = 1.105 m_\odot$ and $m_B = 0.934 m_\odot$, respectively [2] (where m_\odot is the solar mass), while the solar balloon spacecraft represents the massless third body, see Fig. 2.

Both stars rotate around their center of mass C in a period $T = 79.3270$ years. They cover elliptic orbits with the same eccentricity $e = 0.5179$ and semimajor axes μa and $(1 - \mu) a$, respectively, where $a = 23.4$ au [4] and $\mu \triangleq m_B / (m_A + m_B) \approx 0.4581$ is the dimensionless mass of α Cen B. The time-variable distance ℓ between the two stars is [20]

$$\ell = a (1 - e^2) g \quad \text{with} \quad g \triangleq \frac{1}{1 + e \cos \nu} \quad (1)$$

where ν is the true anomaly of α Cen B.

The equation of motion of a massless spacecraft can be written in a rotating and pulsating [20] reference frame $\mathcal{T}_p(C; x/\ell, y/\ell, z/\ell)$ with unit vectors $\hat{\mathbf{i}}$, $\hat{\mathbf{j}}$, and $\hat{\mathbf{k}}$, in which the (x, y) -plane

coincides with the plane of motion of the stars, see Fig. 2. In particular, the x -axis points toward α Cen B at any time instant and rotates around the z -axis with a non-uniform angular velocity $\boldsymbol{\omega} = \omega \hat{\mathbf{k}}$ with

$$\omega = \frac{\sqrt{a (1 - e^2) G (m_A + m_B)}}{\ell^2} \quad (2)$$

where G is the universal gravitational constant.

Let $\boldsymbol{\rho}_A$, $\boldsymbol{\rho}_B$, and \mathbf{r} be the dimensionless position vectors of the solar balloon spacecraft with respect to α Cen A, α Cen B, and C , respectively. According to Szebehely [20], the dimensionless (vectorial) equation of motion of the solar balloon spacecraft is

$$\mathbf{r}'' + 2\hat{\mathbf{k}} \times \mathbf{r}' = g \left[-\frac{1-\mu}{\rho_A^3} \boldsymbol{\rho}_A - \frac{\mu}{\rho_B^3} \boldsymbol{\rho}_B + \frac{\ell^2 \mathbf{a}_P}{G(m_A + m_B)} - \hat{\mathbf{k}} \times (\hat{\mathbf{k}} \times \mathbf{r}) - e \cos \nu (\mathbf{r} \cdot \hat{\mathbf{k}}) \hat{\mathbf{k}} \right] \quad (3)$$

where $\rho_A = \|\boldsymbol{\rho}_A\|$ and $\rho_B = \|\boldsymbol{\rho}_B\|$, whereas the prime symbol denotes a derivative taken with respect to the true anomaly ν .

In Eq. (3), \mathbf{a}_P represents the propulsive acceleration provided by the solar balloon under the effect of the radiation pressure incoming from both α Cen A and B. Assuming that the solar balloon behaves like an ideal spherical solar sail, the resultant propulsive acceleration can be written as the superimposition of the radial acceleration due to each of the two stars, viz.

$$\mathbf{a}_P = \beta \left(\frac{G m_A}{\ell^2 \rho_A^3} \boldsymbol{\rho}_A + \varepsilon \frac{G m_B}{\ell^2 \rho_B^3} \boldsymbol{\rho}_B \right) \quad (4)$$

where $\beta \geq 0$ is a performance parameter, which is referred to as sail lightness number. In this case the sail lightness number is defined as the ratio, calculated at a given distance from α Cen A, between the magnitude of the propulsive acceleration due to the radiation pressure of α Cen A alone and the gravitational acceleration due to α Cen A. Paralleling McInnes [21], for a spacecraft of total mass m with a solar balloon of radius R , the sail lightness number can be written as

$$\beta = \frac{\eta L_A R^2}{2 c G m_A m} \quad (5)$$

where η is the solar sail efficiency that takes into account the optical characteristics of the reflecting surface, $L_A = 1.5190 L_\odot$ is the luminosity (expressed in solar luminosity L_\odot) of α Cen A, and c is the speed of light.

In Eq. (4), the dimensionless parameter ε is a physical property of the binary system, depending on the luminosities and masses of the two stars, and is defined as

$$\varepsilon \triangleq \frac{L_B m_A}{L_A m_B} \approx 0.3896 \quad (6)$$

where $L_B = 0.5002 L_\odot$ [22] is the luminosity of α Cen B. Note that, using Eqs. (6) and (5), the product $\varepsilon \beta$ becomes

$$\varepsilon \beta = \frac{\eta L_B R^2}{2 c G m_B m} \quad (7)$$

In other terms, $\varepsilon \beta$ represents the sail lightness number evaluated using α Cen B as the only radiating body.

2 Analysis of AEPs

Artificial equilibrium points are defined as the equilibrium solutions of Eq. (3). Enforcing the equilibrium conditions [20] $\mathbf{r}'' = 0$ and $\mathbf{r}' = 0$ in Eq. (3), AEPs are the solution of

$$(\beta - 1) \frac{1 - \mu}{\rho_A^3} \boldsymbol{\rho}_A + (\varepsilon \beta - 1) \frac{\mu}{\rho_B^3} \boldsymbol{\rho}_B - \hat{\mathbf{k}} \times (\hat{\mathbf{k}} \times \mathbf{r}) - e \cos \nu (\mathbf{r} \cdot \hat{\mathbf{k}}) \hat{\mathbf{k}} = 0 \quad (8)$$

where Eq. (4), the definitions of μ and \mathbf{a}_P , and the condition $g > 0$ have been taken into account. Equation (8) is a vectorial relationship that links the physical properties of the stars system and the properties of the propulsion system to the positions of the AEPs.

By using the relationships $\boldsymbol{\rho}_B \triangleq \boldsymbol{\rho}_A - \hat{\mathbf{i}}$ and $\mathbf{r} \triangleq \boldsymbol{\rho}_A - \mu \hat{\mathbf{i}}$ among the position vectors, it may be verified that Eq. (8) can be rearranged as [9]

$$d_\rho \hat{\boldsymbol{\rho}}_A = d_i \hat{\mathbf{i}} + d_k \hat{\mathbf{k}} \quad (9)$$

where $\hat{\boldsymbol{\rho}}_A \triangleq \boldsymbol{\rho}_A / \rho_A$, and coefficients d_ρ , d_i , and d_k are defined as a function of only the position vector $\boldsymbol{\rho}_A$ as follows

$$d_\rho = \frac{(\beta - 1)(1 - \mu)}{\rho_A^2} + \frac{(\varepsilon\beta - 1)\mu\rho_A}{\|\boldsymbol{\rho}_A - \hat{\mathbf{i}}\|^3} + \rho_A \quad (10)$$

$$d_i = \mu \left(1 - \frac{1 - \varepsilon\beta}{\|\boldsymbol{\rho}_A - \hat{\mathbf{i}}\|^3} \right) \quad (11)$$

$$d_k = \frac{\boldsymbol{\rho}_A \cdot \hat{\mathbf{k}}}{g} \quad (12)$$

Note that when $\beta = 0$, i.e. a spacecraft without propulsive acceleration, Eq. (8) provides the position of the classical Lagrangian Points L_i with $i = 1 \dots 5$. Also, when $\varepsilon = 0$ the corresponding results coincide with the case of one radiating body only, see Refs. [9,20].

Lastly, note that using the variable distance ℓ as the unit of distance, Eq. (3) describes the motion of the solar balloon spacecraft in the reference frame $\mathcal{T}_p(C; x/\ell, y/\ell, z/\ell)$, which pulsates synchronously to the distance ℓ . This means that an AEP in the pulsating reference frame is at a fixed position \mathbf{r}_0 , whereas it actually oscillates (or pulsates) on a segment of length $2ae\|\mathbf{r}_0\|$ with a period T when seen by an observer in the rotating frame $\mathcal{T}(C; x, y, z)$.

Equation (9) admits two different families of solutions, see Fig. 3. According to the literature, such families of AEPs are referred to as collinear and triangular points. In particular, the collinear AEPs are partitioned in three groups, i.e. L_1 -type, L_2 -type, and L_3 -type, see Fig. 3. Both families belong to the (x, y) -plane (that is, $d_k = 0$). In fact, were $d_k \neq 0$, Eq. (8) would be ν -dependent [see also Eqs. (9) and (12)], and so would be any solution, which is in contrast with the equilibrium conditions. Similar considerations apply in case of a single radiating body, see [13]. Moreover, Eq. (9), which involves the points in the (x, y) -plane, does not depend on the eccentricity of the system and is formally equal to the corresponding equation for the circular photogravitational problem. Therefore, the results involving the position of AEPs in the pulsating reference frame formally coincide with those of the circular problem, in particular with some results

reported in Simmons et al. [14].

2.1 Collinear AEPs

Collinear AEPs are obtained by setting $d_k = 0$, $d_\rho \neq 0$, and $d_i \neq 0$ in Eq. (9). In this case, the AEPs are aligned with the x -axis (i.e. $\hat{\boldsymbol{\rho}}_A \cdot \hat{\mathbf{i}} = \pm 1$) and

$$d_\rho = d_i \hat{\boldsymbol{\rho}}_A \cdot \hat{\mathbf{i}} \quad (13)$$

From Eqs. (10), (11) and (13), the sail lightness number required to maintain an AEP at a given position $\boldsymbol{\rho}_{A_0} = \rho_{A_0} (\hat{\boldsymbol{\rho}}_{A_0} \cdot \hat{\mathbf{i}}) \hat{\mathbf{i}}$, is

$$\beta_0 = \frac{\frac{\mu \rho_{A_0}^2}{(1-\mu) \hat{\boldsymbol{\rho}}_{A_0} \cdot \hat{\mathbf{i}}} \left(1 + \frac{\rho_{A_0} \hat{\boldsymbol{\rho}}_{A_0} \cdot \hat{\mathbf{i}} - 1}{\|\rho_{A_0} \hat{\boldsymbol{\rho}}_{A_0} \cdot \hat{\mathbf{i}} - 1\|^3} \right) - \frac{\rho_{A_0}^3}{1-\mu} + 1}{1 + \frac{\varepsilon \mu \rho_{A_0}^2 (\rho_{A_0} \hat{\boldsymbol{\rho}}_{A_0} \cdot \hat{\mathbf{i}} - 1)}{(1-\mu) \hat{\boldsymbol{\rho}}_{A_0} \cdot \hat{\mathbf{i}} \|\rho_{A_0} \hat{\boldsymbol{\rho}}_{A_0} \cdot \hat{\mathbf{i}} - 1\|^3}} \quad (14)$$

where we used the fact that $\rho_B = \|\rho_A \hat{\boldsymbol{\rho}}_A \cdot \hat{\mathbf{i}} - 1\|$.

Figure 4(a) shows the values of β_0 as a function of the position of collinear points along x -axis. Because β cannot be negative, only a subset of points of x -axis (gray regions in figure) corresponds to feasible equilibrium points. When $\beta_0 = 0$ (zero propulsive acceleration), the three classical collinear Lagrangian points are recovered. Increasing β_0 up to 1, the position of the three collinear AEPs moves towards the two stars. When $\beta_0 > 1$ the L_3 -type AEP passes through the α Cen A position and becomes an L_1 -type point. In that case two L_1 -type points and one L_2 -point exist up to $\beta_M \approx 1.0006$, where the two L_1 -type points coalesce, see point M at $\rho_{A_0} \approx 0.0721$ in Figs. 3 and 4(a).

Beyond that value, L_1 -type points also disappear, and only one L_2 -type point exists until $\beta_0 = 1/\varepsilon \approx 2.5668$ is reached. At this value, L_2 -type AEP becomes a L_1 -type point which moves toward the point P_2 (see also Fig. 3) at $\rho_{A_0} \approx 0.6354$ (where the denominator of Eq. (14)

becomes zero) as β_0 tends to infinity. Note that for $\varepsilon = 0$, P_2 would coincide with α Cen B, and M would coincide with α Cen A for a value $\beta_M = 1$. This result is consistent with Ref. [9].

2.2 Triangular AEPs

Triangular AEPs are obtained when conditions $d_\rho = 0$, $d_i = 0$, and $d_k = 0$ are met. Such points are constrained to lie in the (x, y) -plane and form a triangle with the two stars. For an equilibrium point at a given distance ρ_{A_0} from α Cen A, in order to met the condition $d_i = 0$, the equilibrium point must be at a distance from α Cen B given by

$$\rho_{B_0} = (1 - \varepsilon \beta_0)^{1/3} \quad (15)$$

where β_0 is the sail lightness number required to maintain that equilibrium point. The value of β_0 is given by the condition $d_\rho = 0$, viz.

$$\beta_0 = 1 - \rho_{A_0}^3 \quad (16)$$

Note that Eqs. (15) and (16) are consistent with the results of Ref. [15].

Figure 4(b) shows both β_0 and ρ_{B_0} as functions of ρ_{A_0} . As in the case of collinear points, for $\beta_0 = 0$ the classical equilateral points ($\rho_{A_0} = \rho_{B_0} = 1$) are recovered. The triangular AEPs move towards the x -axis as long as β_0 is increased up to the value $\beta_{\max} \approx 0.9965$, in correspondence of which the equilateral points coalesce with the collinear points (point P_1 at $\rho_{A_0} \approx 0.1511$ in Fig. 3). The value β_{\max} is the solution of the equation

$$(1 - \beta_{\max})^{1/3} + (1 - \varepsilon \beta_{\max})^{1/3} = 1 \quad (17)$$

corresponding to the condition $\rho_{A_0} + \rho_{B_0} = 1$. Note that when $\varepsilon = 0$, β_{\max} is equal to 1 and P_1 coincides with α Cen A, according to Ref. [9].

3 Linear Stability and Control of AEPs

The dynamics around an AEP generated by means of a solar balloon spacecraft is now better characterized by analyzing the linear stability and the possibility of control. Note that a linear analysis only provides necessary conditions for nonlinear stability and sufficient conditions for instability, therefore also simulations of the nonlinear dynamics are provided to confirm the results of the linear analysis.

The linear stability of AEPs in the neighborhood of the equilibrium points is studied by linearizing Eq. (3) around the equilibrium position \mathbf{r}_0 , obtained using a solar balloon with a sail lightness number equal to β_0 . Assume that a given AEP may be controlled using a suitable variation of β , that is, by means of a so called β -control [12]. From a design point of view, a β -control can be achieved with an active control strategy that uses either an inflating and deflating mechanism of the balloon, or through variable reflectance materials mounted on the balloon's surface.

The linearized equation of motion of the solar balloon spacecraft is obtained by using the transformation $\mathbf{r} = \mathbf{r}_0 + \delta\mathbf{r}$ and $\beta = \beta_0 + \delta\beta$, and introducing the second-order tensors \mathbf{K} , \mathbf{E} , and the vector \mathbf{u} defined as

$$\mathbf{K} = \nabla \left[(\beta - 1) \frac{1 - \mu}{\rho_A^3} \boldsymbol{\rho}_A + (\varepsilon \beta - 1) \frac{\mu}{\rho_B^3} \boldsymbol{\rho}_B - \hat{\mathbf{k}} \times (\hat{\mathbf{k}} \times \mathbf{r}) - e \cos \nu (\mathbf{r} \cdot \hat{\mathbf{k}}) \hat{\mathbf{k}} \right] \Big|_{\mathbf{r}_0, \beta_0} \quad (18)$$

$$\mathbf{E} \cdot \mathbf{r} = \hat{\mathbf{k}} \times \mathbf{r} \quad (19)$$

$$\mathbf{u} = \frac{\partial}{\partial \beta} \left(\beta \frac{1 - \mu}{\rho_A^3} \boldsymbol{\rho}_A + \varepsilon \beta \frac{\mu}{\rho_B^3} \boldsymbol{\rho}_B \right) \Big|_{\mathbf{r}_0, \beta_0} \quad (20)$$

The resulting system of differential equation is [12,20]

$$\frac{d}{d\nu} \begin{bmatrix} \delta \mathbf{r} \\ \delta \mathbf{r}' \end{bmatrix}_{\mathcal{T}_p} = \begin{bmatrix} \mathbb{O}_{3 \times 3} & \mathbb{I}_{3 \times 3} \\ g \mathbb{K}^T & -2 \mathbb{E} \end{bmatrix} \begin{bmatrix} \delta \mathbf{r} \\ \delta \mathbf{r}' \end{bmatrix}_{\mathcal{T}_p} + \begin{bmatrix} \mathbb{O}_{3 \times 1} \\ g \mathbb{U} \end{bmatrix} \delta \beta \quad (21)$$

where $\mathbb{O}_{n \times m}$ and $\mathbb{I}_{n \times m}$ are zero and identity n -by- m matrices, whereas \mathbb{K} , \mathbb{E} , and \mathbb{U} are matrices whose entries are the components of \mathbf{K} , \mathbf{E} , and \mathbf{u} in the rotating frame \mathcal{T}_p .

Equation (21) represents a system of linear, non-autonomous, differential equations with 2π -periodic coefficients due to the presence of the parameter g , see Eq. (1). Therefore, the linear stability analysis around an equilibrium point may be addressed with the aid of Floquet theory [23]. As long as $\delta\beta = 0$, an analysis of Eq. (21) shows that the AEPs obtained with a solar balloon in the α Centauri system are, in general, unstable. This result is by no means surprising, since the classical equilibrium points are unstable (due to the high values of both μ and e [20]), and the solar balloon propulsive acceleration does not produce a stabilizing effect. Despite that, AEPs may be stabilized, provided that a suitable control strategy is introduced.

Before showing the effects of a control strategy, it should be noted that the system described by Eq. (21) is not fully controllable. In fact, the linearized motion along the z -axis is uncoupled from that in the (x, y) -plane (where the AEPs lie) and is not affected by the control $\delta\beta$. As a result, the motion along z cannot be controlled. However, equilibrium points may still be stabilizable, if the linearized motion along z turns out to be stable.

The following stability analysis will be focused on the L_1 -type AEPs that lie between α Cen A and the classical L_1 point ($\rho_{A_{L_1}} = 0.5173$). Such AEPs are very interesting for observational missions because they lie between the two stars, thus enabling simultaneous observations of both of them. Moreover, these points require small values of β_0 , if generated close to L_1 , and they may be stabilized with a simple control law, as is shown next.

For L_1 -type point ($\hat{\rho}_{A_0} \cdot \hat{\mathbf{i}} = 1$, $\rho_{B_0} = 1 - \rho_{A_0}$), matrix \mathbb{K} and vector \mathbb{U} defined by Eqs. (18) and (20) become

$$\mathbb{K} = \begin{bmatrix} -2k_{22} + 3 & 0 & 0 \\ 0 & k_{22} & 0 \\ 0 & 0 & k_{22} - 1 \end{bmatrix}, \quad \mathbb{U} = \begin{bmatrix} \frac{1 - \mu}{\rho_{A_0}^2} - \frac{\varepsilon\mu}{(1 - \rho_{A_0})^2} \\ 0 \\ 0 \end{bmatrix} \quad (22)$$

where

$$k_{22} = 1 + \frac{(\beta_0 - 1)(1 - \mu)}{\rho_1^3} + \frac{\mu(\varepsilon\beta_0 - 1)}{(1 - \rho_1)^3} \quad (23)$$

and β_0 is given by Eq. (14).

With the aim of stabilizing the equilibrium point, introduce now a PD feedback control law for the x component in the form

$$\delta\beta = -h_P (\delta\mathbf{r} \cdot \hat{\mathbf{i}}) - h_D (\delta\mathbf{r}' \cdot \hat{\mathbf{i}}) \quad (24)$$

with h_P and h_D being the proportional and derivative gains, respectively. A Floquet analysis of the system (21) with \mathbb{K} and \mathbb{U} given in Eq. (22), and $\delta\beta$ defined in Eq. (24), provides the values of the gains h_P and h_D required for the stabilization of a given L_1 -type AEP at a distance ρ_{A_0} from α Cen A.

Figure 5(a) illustrates the values of the gains under the assumption that $h_P = h_D$. The regions in which the linearized dynamics of AEPs is unstable are highlighted in gray color. In particular, note the small stripe (placed at $\rho_{A_0} \approx 0.2759$) where instability originates from an unstable dynamics along z -axis. Figure 5(b) shows the value of pairs (h_P, h_D) necessary to stabilize the point located at $\rho_{A_0} = 0.5$. Independent of h_D , the AEP turns out to be stable for $h_P > 10.1$.

Numerical simulations of Eq. (3) confirm the results of Fig. 5. For example, Fig. 6 shows the effects of a PD control on the L_1 -type point at $\rho_{A_0} = 0.5$, which is the point maintained by a

solar balloon spacecraft with $\beta_0 = 0.2019$. Note that the selected AEP lies always in the middle of the segment between α Cen A and B, see Fig. 6(a), both in the synodic frame $\mathcal{T}(C; x, y, z)$ and in the pulsating frame $\mathcal{T}_p(C; x/\ell, y/\ell, z/\ell)$. In this sense, the point with $\rho_{A_0} = 0.5$ allows the spacecraft to observe both the stars at the same relative distance. Moreover, the selected collinear point is stabilizable with a β control, as the linearized motion along z turns out to be stable according to Fig. 5. For that AEP, the required value of β_0 corresponds to a ratio $R^2/m = 30.46 \text{ m}^2/\text{kg}$ in case of a perfectly reflecting solar balloon surface. This means that a spacecraft of total mass $m = 100 \text{ kg}$ (including the solar balloon mass) requires a balloon radius of about 55 m. On the other hand, a spacecraft with a mass of 200 kg would require a balloon radius of about 78 m in order to maintain the same AEP. For example, the NASA satellite ECHO 1 [24], which was launched on August 1960, was essentially a spherical solar sail (inflated balloon) with a nominal diameter of about 30 m.

Figure 6(b) gives the trajectories in $\mathcal{T}(C; x, y, z)$ over a time span equal to T and assuming initial spacecraft position and velocity errors of 30000 km and of 270 m/s, respectively. The thick continuous line in figure corresponds to the nominal AEP in the unperturbed case. Note how the AEP is actually a segment of length $2ae(\rho_{A_0} - \mu) \approx 1.0163 \text{ au}$. The dashed line corresponds to the uncontrolled case, which is unstable according to Fig. 5. The solid line refers to a controlled case with $h_P = h_D = 15$ (stable case, according to Fig. 5), whereas the dash-dot line concerns to a situation in which the gains ($h_P = h_D = 5$) are unable to guarantee stability. For the stable case, the variation of β (as percentage of β_0) required to control the AEP is shown in Fig. 6(c). Note that the considerable value of $\delta\beta/\beta_0$ at the beginning of the simulation, i.e. $|\delta\beta/\beta_0| \simeq 75\%$ for $\nu = 0$, is essentially due to the high values of the initial position and velocity errors.

4 Conclusions

The propulsive acceleration of a solar balloon spacecraft represents an effective way to displace the equilibrium points of the α Centauri A and B binary system. Two families of artificial equilibrium points may be generated, at which a spacecraft can be placed depending on the amount of available propulsive acceleration. These equilibrium points belong to the plane of motion of the two stars. Even though these equilibrium points are unstable, a linearized analysis of L_1 -type points shows that most of them may be stabilized by means of a proportional-derivative feedback control law. Such a conclusion is also strengthened by numerical simulations of the complete non-linear dynamics of the three-body system. These results can be used as first order estimates of the requirements of a candidate mission around an equilibrium point for a future observation mission of the α Centauri A and B binary system. Current research involves the development of a more refined model that takes into account the effects of Proxima and includes other nonlinear phenomena such as control system delay and saturation.

Acknowledgments

This research project has been developed within MIRA Collaboration, a no-profit joint scientific work regarding a future stellar sailcraft carried to a nearby star by a starship, hopefully launched at the end of 21st-century towards the high-rank-of-exploration system of Alpha Centauri. This collaboration currently involves Italian universities (University of Rome “La Sapienza” and University of Pisa), and is open to other national and international entities. The project coordinator is Dr. Giovanni Vulpetti.

References

- [1] J. G. Wertheimer, G. Laughlin, Are Proxima and Alpha Centauri gravitationally bound?, *The Astronomical Journal* 132 (5) (2006) 1995–1997, doi: 10.1086/507771.
- [2] G. F. Porto de Mello, W. Lyra, G. R. Keller, The Alpha Centauri binary system. atmospheric parameters and element abundances, *Astronomy and Astrophysics* 488 (2) (2008) 653–666, doi: 10.1051/0004-6361:200810031.
- [3] J. M. Guedes, E. J. Rivera, E. Davis, G. Laughlin, E. V. Quintana, D. A. Fischer, Formation and Detectability of Terrestrial Planets around α Centauri B, *The Astrophysical Journal* 679 (2) (2008) 1582–1587, doi: 10.1086/587799.
- [4] F. Duncan, Oscillations in the habitable zone around α Centauri B, *Monthly Notices of the Royal Astronomical Society* 422 (2) (2012) 1241–1249, doi: 10.1111/j.1365-2966.2012.20698.x.
- [5] X. Dumusque, F. Pepe, C. Lovis, D. Segransan, J. Sahlmann, W. Benz, F. Bouchy, M. Mayor, D. Queloz, N. Santos, S. Udry, An Earth-mass planet orbiting α Centauri B, *Nature* 491 (7423) (2012) 207–211, doi: 10.1038/nature11572.
- [6] P. A. Wiegert, M. J. Holman, The Stability of Planets in the Alpha Centauri system, *Astronomical Journal* 113 (4) (1997) 1445–1450, doi: 10.1086/118360.
- [7] C. Circi, Properties of transit trajectory in the restricted three and four-body problem, *Advances in Space Research* 49 (10) (2012) 1506–1519, doi: 10.1016/j.asr.2012.02.034.
- [8] C. Circi, P. Teofilatto, Effect of planetary eccentricity on ballistic capture in the solar system, *Celestial Mechanics and Dynamical Astronomy* 93 (1-4) (2005) 69–86, doi: 10.1007/s10569-005-3640-9.
- [9] G. Aliasi, G. Mengali, A. A. Quarta, Artificial equilibrium points for a generalized sail in the elliptic restricted three-body problem, *Celestial Mechanics and Dynamical Astronomy* 114 (1-2) (2012) 181–200, doi: 10.1007/s10569-012-9425-z.

- [10] R. J. McKay, M. Macdonald, J. Biggs, C. McInnes, Survey of highly-non-keplerian orbits with low-thrust propulsion, *Journal of Guidance, Control, and Dynamics* 34 (3) (2011) 645–666, doi: 10.2514/1.52133.
- [11] C. Circi, Three-axis attitude control using combined gravity-gradient and solar pressure, *Proceedings of the Institution of Mechanical Engineers, Part G: Journal of Aerospace Engineering* 221 (1) (2007) 85–90, doi: 10.1243/09544100JAERO48.
- [12] J. D. Biggs, C. R. McInnes, Passive orbit control for space-based geo-engineering, *Journal of Guidance, Control and Dynamics* 33 (3) (2010) 1017–1020, doi: 10.2514/1.46054.
- [13] H. Baoyin, C. R. McInnes, Solar sail equilibria in the elliptical restricted three-body problem., *Journal of Guidance, Control, and Dynamics* 29 (3) (2006) 538–543, doi: 10.2514/1.15596.
- [14] J. F. L. Simmons, A. J. C. McDonald, J. C. Brown, The restricted 3-body problem with radiation pressure, *Celestial Mechanics* 35 (2) (1985) 145–187., doi: 10.1007/BF01227667.
- [15] V. V. Markellos, E. Perdios, P. Labropoulou, Linear stability of the triangular equilibrium points in the photogravitational elliptic restricted problem, I, *Astrophysics and Space Science* 194 (2) (1992) 207–213, doi: 10.1007/BF00643991.
- [16] V. V. Markellos, E. Perdios, C. Georgiou, Linear stability of the triangular equilibrium points in the photogravitational elliptic restricted problem, II, *Astrophysics and Space Science* 199 (1) (1993) 23–33, doi: 10.1007/BF00612974.
- [17] V. V. Markellos, E. Perdios, K. Papadakis, The stability of inner collinear equilibrium points in the photogravitational elliptic restricted problem, *Astrophysics and Space Science* 199 (1) (1993) 139–146, doi: 10.1007/BF00612984.
- [18] G. Aliasi, G. Mengali, A. A. Quarta, Artificial lagrange points for solar sail with electrochromic material panels, In Press. *Journal of Guidance, Control and Dynamics*doi: 10.2514/1.58167.
- [19] G. Aliasi, G. Mengali, A. A. Quarta, Passive control feasibility of collinear equilibrium points with solar balloons, *Journal of Guidance, Control, and Dynamics* 35 (5) (2012) 1657–1661, doi: 10.2514/1.57393.

- [20] V. Szebehely, Theory of orbits: the restricted problem of three bodies, Academic Press, New York, 1967, pp. 587–602.
- [21] C. R. McInnes, Solar Sailing: Technology, Dynamics and Mission Applications, Springer, Berlin, 1999, Ch. 2, 3, pp. 34–40, 56–60, ISBN: 1-852-33102-X.
- [22] F. Thévenin, J. Provost, P. Morel, G. Berthomieu, F. Bouchy, F. Carrier, Asteroseismology and calibration of α cen binary system, *Astronomy & Astrophysics* 392 (1) (2002) L9–L12, doi: 10.1051/0004-6361:20021074.
- [23] J. K. Hale, Ordinary differential equations, Dover Publications, Inc., 1980, Ch. 8, pp. 117–121, 280, ISBN: 0-486-47211-6.
- [24] D. O. Muhlemann, R. H. Hudson, D. Holdridge, R. L. Carpenter, K. Oslund, Observed Solar Pressure Perturbations of Echo I, *Science, New Series*, 132 (3438) (1960) 1487, doi: 10.1126/science.132.3438.1487.

List of Figures

1	Schematic view of the α Centauri system (dimensions of stars are to scale [2]).	21
2	Solar balloon spacecraft within the α Cen A and B binary star system.	22
3	Families of AEPs for a solar balloon spacecraft in the α Cen A and B system. Arrows indicate that β increases, see also Fig. 4.	23
4	Sail lightness number as a function of the position of AEPs in the rotating frame.	24
5	Stability maps for L_1 -type points.	25
6	Simulations for perturbed L_1 -type AEP at $\rho_{A_0} = 0.5$ with and without control.	26

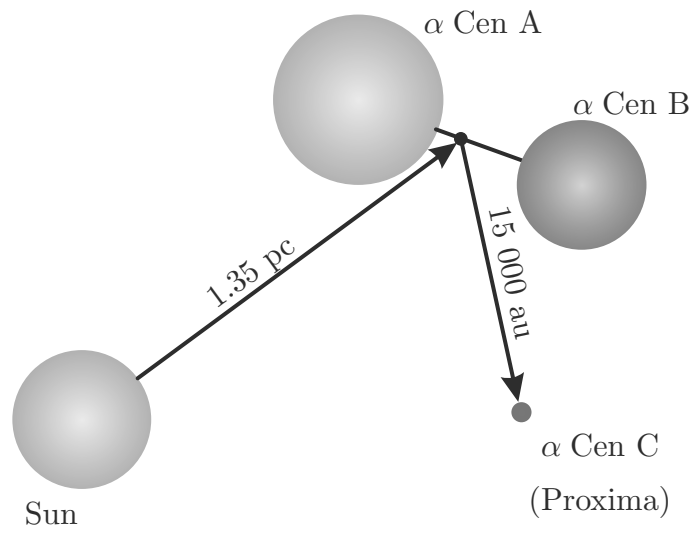


Figure 1. Schematic view of the α Centauri system (dimensions of stars are to scale [2]).

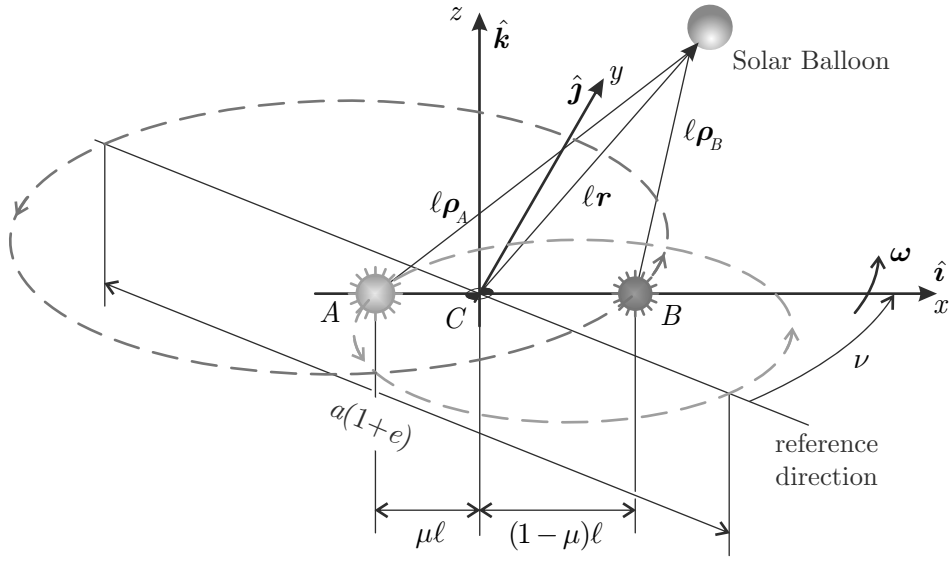


Figure 2. Solar balloon spacecraft within the α Cen A and B binary star system.

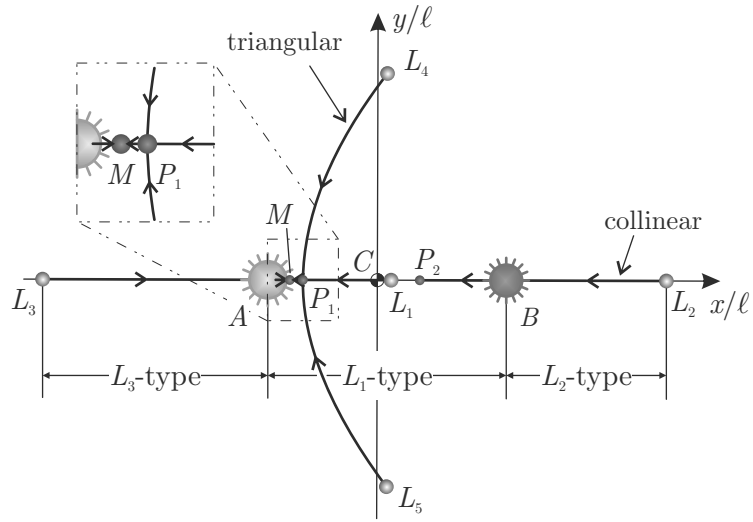
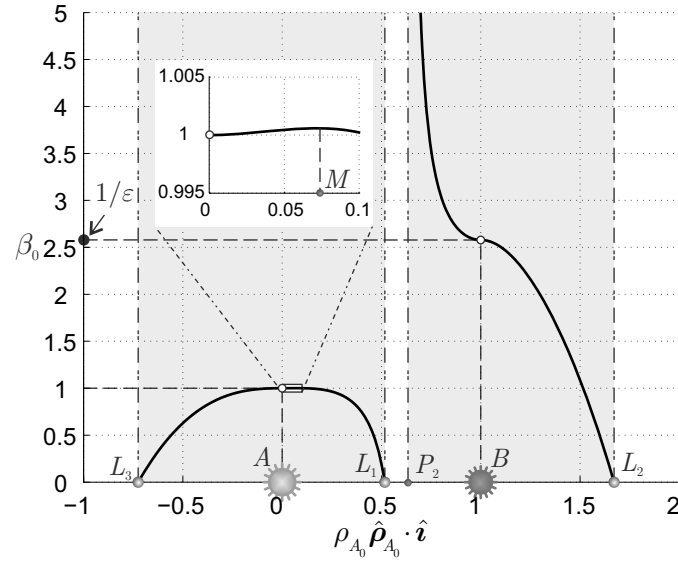
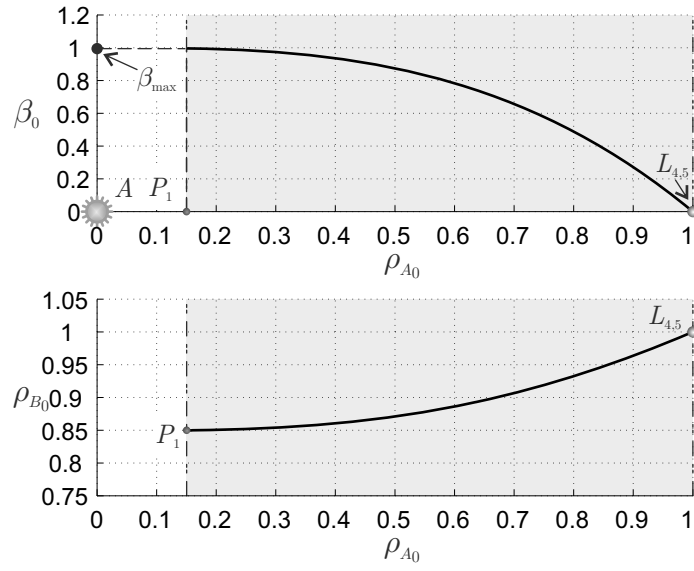


Figure 3. Families of AEPs for a solar balloon spacecraft in the α Cen A and B system. Arrows indicate that β increases, see also Fig. 4.

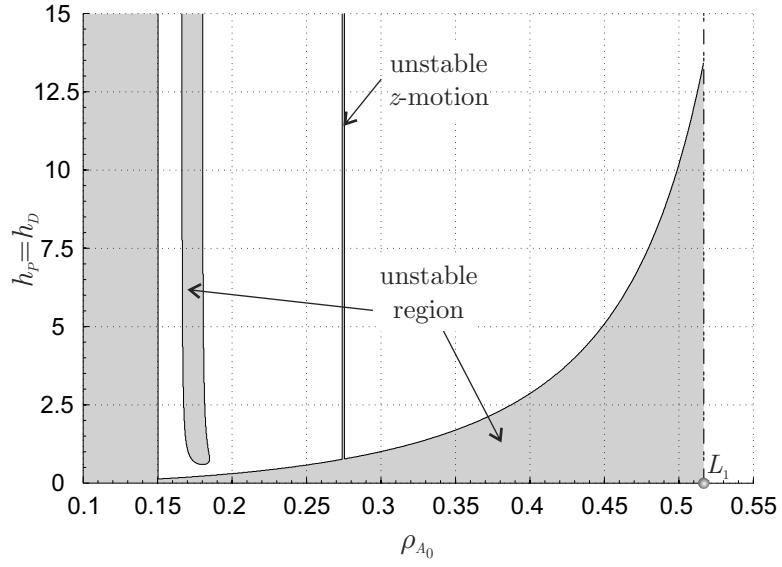


(a) Collinear AEPs.

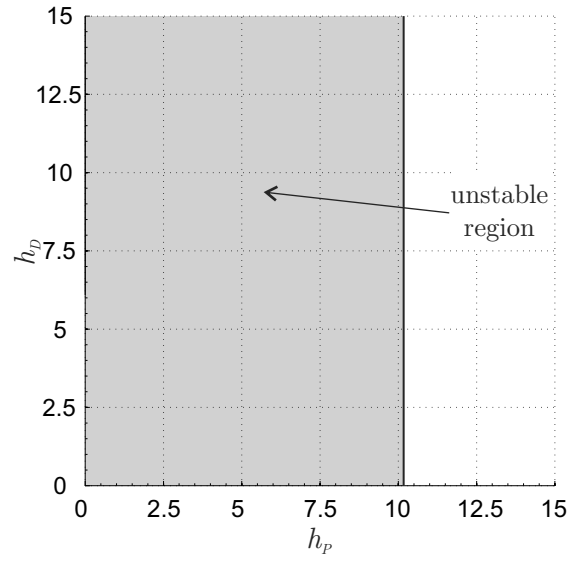


(b) Triangular AEPs.

Figure 4. Sail lightness number as a function of the position of AEPs in the rotating frame.



(a) Map with $h_P = h_D$



(b) Map for $\rho_{A_0} = 0.5$

Figure 5. Stability maps for L_1 -type points.

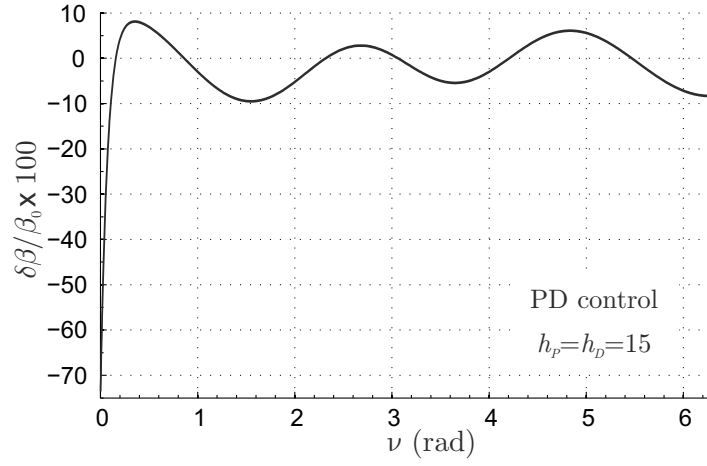
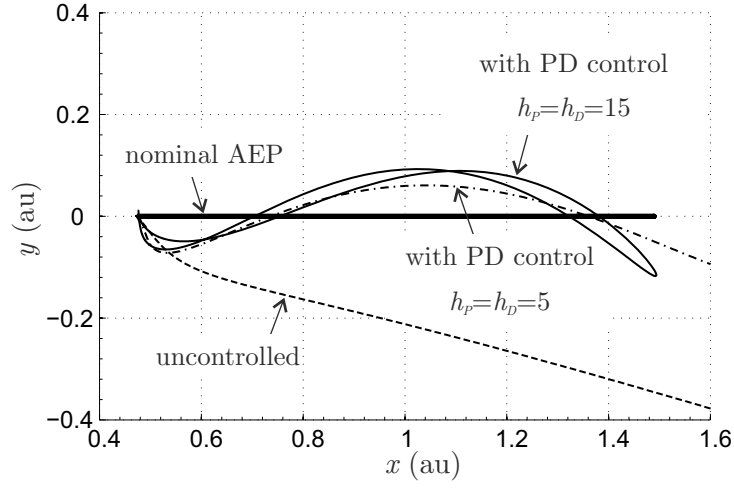
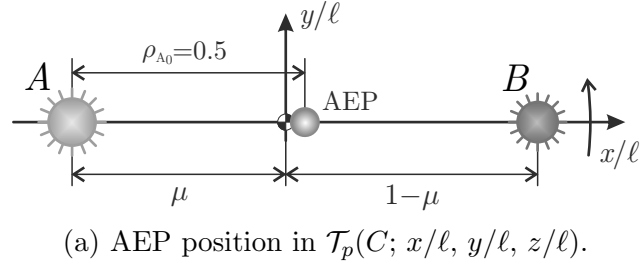


Figure 6. Simulations for perturbed L_1 -type AEP at $\rho_{A_0} = 0.5$ with and without control.